Journal of Engineering Science and Technology
Vol. 17, No. 4 (2022) 2412 - 2430

NUMERICAL INVESTIGATION OF DIESEL ENGINE PERFORMANCE OPERATED IN DUAL FUEL PHASE WITH INCREASING SYNGAS DIESEL ADDITION RATIO AND LAMBDA VALUE OF 1

HUSSEIN A. MAHMOOD[1,*], ALI O. AL-SULTTANI[2], ALI I. MOSA[3]

[1]Department of Reconstruction and projects, University of Baghdad, Baghdad, Iraq
[2]Department of Water Resources Engineering, College of Engineering, University of Baghdad, Baghdad, Iraq
[3]Mechanical Engineering Department, College of Engineering, University of Baghdad, Jadriyah - Baghdad, Iraq
*Corresponding Author: husseinadel@uobaghdad.edu.iq

Abstract

Syngas is one of the most promising alternative fuels that researchers have recently been focusing on in the field of dual fuel technology. Only a Few scientists have attempted to substitute diesel fuel with syngas fuel. As a result, essential knowledge on mixing ratios, combustion characteristics, and pollution from diesel-syngas dual fuel engines remains limited. In this simulation study, Fluent software 16.1 was used to evaluate the emissions as well as the combustion properties of a diesel-syngas mixture at dual fuel mode under different addition ratios of syngas with diesel, 2000 rpm engine speed, and lambda value of 1. The numerical simulations have been conducted on single cylinder diesel engine that operates using the direct injection technique. In addition, an increase was indicated via the results in peak temperature and pressure when syngas fuels were added and directly influenced by H_2 percentage. Based on the results, increasing the fraction of diesel fuel in the mixture limits the increase of Nitric oxide (NO), Carbon dioxide (CO_2) and Carbon monoxide (CO) emissions, due to the low flammability of diesel combustion. While rising the syngas percentage in the mixture increases emissions of NO, CO_2, and CO. due to the syngas has a fast-burning level, in turn leads to the high combustion temperature for the mixture.

Keywords: Addition ratio, Computational fluid dynamics (CFD), Lambda; Combustion, Syngas Diesel dual fuel engine.

1. Introduction

There is a rapid increase in terms of energy use in today's modern world, in which novel technologies were introduced constantly. Also, fossil fuel, especially petroleum fuel, can be defined as the main energy production contributor [1]. The consumption of fossil fuel was rising steadily due to enhancements in living standards and the growth of the population. Increased production of fuel is essential to increase the energy demands, therefore draining the present reserve levels of fossil fuels at fast rates [2]. Approximately 60% of current oil reserves in the world are considered to be in regions which were in constant political chaos. This led to fluctuating prices of oil and supply disruptions [1, 3].

Worldwide, the majority of used energy was supplied via fossil fuels. Waste materials are generated via fossil fuels' burning, majorly emissions into the atmosphere as dust and combustion fuel gases, along with a few clinkers and/or ash. Soot particles, carbon monoxide, oxides of nitrogen, oxides of Sulphur, and hydrocarbon are the emissions produced from internal engine combustion. Those emissions species are undesirable since they give detrimental impacts on the atmosphere and human well-being [4-6]. The rapid depletion of fossil fuels and increasing the increase in global awareness regarding protecting the environment and human are forcing engine manufacturers to search for new alternatives that are reliable, and environmentally friendly fuel. Alternate fuels, including blend of hydrogen and Compressed natural gas (HCNG), Compressed natural gas (CNG), Liquefied natural gas (LNG), Liquefied petroleum gas (LPG), biomass, bio-diesel, ethanol, hydrogen, producer gas, methanol, and syngas, were attempted all over the world [1, 7].

Among these alternative fuels, syngas shows great potential. Synthesis gas (syngas) is considered as a direct end-product related to the gasification process of the bio as well as fossil fuels [8, 9]. In addition, syngas can be defined as one of the gaseous fuels consisting of combustible constituents which majorly comprises of hydrogen (H_2), Carbon monoxide CO, and methane (CH_4) along with non-combustible constituents comprising Carbon dioxide (CO_2), nitrogen (N_2), and water (H_2O). Also, there is a possibility for finding different percentages of H_2, CO, CO_2, CH_4, H_2O, and N_2 in the syngas composition. Because of its high self-ignition temperature, the syngas might not be utilized alone for the purpose of running a compression ignition (CI) diesel engine; thus, it was utilized via dual fuel operation mode [10-12].

The syngas fuel is one of the alternative fuels that is suitable to operating with dual-fuel engines with the lean mixture so that diesel as pilot fuel and the Syngas is the main fuel. There are few fuels that do not have enough ignition characteristics for enabling ignition; therefore, two fuels should be utilized [11, 13]. Primary fuel's ignition (generally gaseous) was activated via in-cylinder conditions. In such a condition, initially, the pilot diesel fuel will be injected, leading to ignition and increasing the combustion chamber's temperature [14]. After that, a primary gaseous fuel, that is considered to be syngas in this condition, was ignited with the increase in the temperature of the chamber, with the following combustion. In addition, the dual-fuel engines were utilized for various applications to use the gaseous fuel types. They have been majorly modified diesel engines and might be achieving extremely low levels of emission, especially for particulates and smoke. The advantages of dual fuel conversion involve quieter and smoother operations,

fuel savings, considerable long engine life between the overhauls, and improved safety [14, 15]. Only a Few scientists have attempted to substitute diesel fuel with syngas fuel. As a result, essential research on mixing ratios, combustion characteristics, and pollution from diesel-syngas dual-fuel engines remains limited. The goal of this research is to examine the combustion properties of syngas-diesel for dual-fuel engines with a lambda value of 1 and five different syngas-diesel addition ratios (10% to 50%).

2. Engine Test Setup and Test Procedure

The engine specifications and gaseous fuel properties are presented in Tables 1 and 2. In this research, the engine has been operated under diesel engine and dual fuel mode with engine speed 2000 rpm and lambda value of 1. Diesel-syngas dual-fuel mode was selected in this study. Because of knocking, the maximum addition ratio was limited to 50% [13]. Adding the syngas fuel into a diesel engine demands different techniques in order to identify the dual operation. Those techniques include carburetion, continuous manifold induction, direct injections, and timing-controlled manifold/port injection. In the present work, the diesel has been injected (in a direct way) in the cylinder, and the syngas fuel was noticeably aspirated into the intake port in combination with air. Hence, the syngas fuels have been recognized as a mass fraction of the air in FLUENT. Furthermore, the cylinder's fresh air consisted of nitrogen (N_2)and oxygen (O_2)with a mass fraction of 76.8% and 23.2%, then the subsequent expression was used for presenting a mass fraction of air, and syngas [16-18].

$$\text{Addition ratio } \% = \frac{\dot{m}_S \, x \, LHV_S}{\dot{m}_D \, x \, LHV_D + \dot{m}_S \, x \, LHV_S} * 100\% \quad (1)$$

where $\dot{m}_D$ and $\dot{m}_S$ were the mass flow rates related to diesel as well as syngas fuels in kg/h. LHV_S and LHV_D were the lower values of heating that are related to diesel and syngas in MJ/kg (Table 2). The mass fraction of syngas in the air was presented in Table 3.

Table 1. Engine description [19, 20].

Engine type	diesel
Model	Ricardo Hydra
Number of cylinders	1
Valve Number	2
Stroke (mm)	88.9
Bore (mm)	80.26
Swept volume (lit)	0.45
Combustion chamber shape	bowl in piston
Compression ratio	20.36

Table 2. Properties of fuels [21, 22].

	Syngas	**Diesel**
Auto ignition temperature (K)	873-923	477-533
Flammability limits (Vol% in air)	6-74	0.7-5
LHV(MJ/kg)	50.02	42.8
Stoichiometric AFR	4.58	14.5
Density (kg/m^3)	0.60565	833-881

Table 3. Mass fraction of syngas, O_2, and N_2. (Lambda value =1).

Type of blending	Addition ratio by energy	Oxygen Mass fraction X 100	Nitrogen Mass fraction X 100	syngas Mass fraction X 100
Diesel	0%	0.233	0.767	0
Diesel-syngas	20 %	0.2241890	0.737995	0.0378151
	30%	0.2209399	0.727300	0.0517598
	40%	0.2168983	0.713995	0.0691056
	50%	0.2125776	0.699772	0.0876494

3. Model Development and Numerical Setup

There are extremely complicated physical phenomena related to combustion flow in internal combustion engines. In this research, Ansys fluent software was used to simulate the combustion under the dual-fuel phase which included unsteady flow with turbulence effects. The numerical method is one of the segregated pressure-based solution algorithms. To solve the species, a discrete phase injection with the species transport equation as well as finite rate chemistry reactions was utilized. In addition, the upwind scheme has been used for the model equation's discretization. FLUENT applies a control volume-based approach for converting governing equations into algebraic ones, which might solve numerically. Furthermore, governing equations in terms of momentum, mass, and energy equations are utilized, also suitable initial boundary conditions are selected for the combustion analysis. ANSYS is on the basis of the approach of pressure correction, and it applies the PISO algorithm. A 2nd-order upwind differencing (UD) method was utilized for momentum, turbulence, and energy equations [23-26].

3.1. Turbulence model

Turbulence was differentiated via velocity field fluctuation. In the presented study, a common RNG kε model was utilized for modeling the turbulence according to [19, 23]. Also, RNG kε model is obtained with the use of a detailed statistical approach. It is considered to be analogous in a form to the standard kε model, yet has a benefit to include the swirl's effect, which was significant for ICE combustion analysis.

3.2. Spray breakup model

FLUENT provides 2 models of the spray breakup, wave, and TAB model. The latter is used in this study; it is on the basis of an analogy between the oscillating as well as distorting droplet and spring-mass system. This study implements the distorting droplet impact [27].

3.3. Ignition delay (autoignition) modeling

In terms of this work, the autoignition (also referred to as Harden burg) model [28] is vital and adequate to simulate a direct injection Diesel engine. In addition, the autoignition was developed with using transport equations for specific ignition species, Yig (Fluent, 2006) that is indicated as follows [27, 28]:

$$\frac{\partial \rho Y_{ig}}{\partial t} + \nabla.\left(\rho \vec{v} Y_{ig}\right) = \nabla.\left(\frac{\mu_t}{Sc_t}\nabla Y_{ig}\right) + \rho S_{ig} \quad (2)$$

where *Yig* is the mass fraction of a radical species, S_{ig} is the source term for the ignition species, *Sct* is turbulent Schmidt number, ρ is the fluid density (kg/m^3), v is the absolute velocity vector (m/s), and μt is the viscosity

3.4. Species transport equations

ANSYS FLUENT estimates the local mass fraction of each species, Y_i, by solving a convection-diffusion equation for the ith species when users select to solve conservation equations for chemical species. The following is the general version of the conservation equation:

$$\frac{\partial}{\partial t}(\rho Y_i) + \nabla.(\rho \vec{v} Y_i) = -\nabla.\vec{J_i} + R_i + S_i \tag{3}$$

where *Yi* =mass fraction of a chemical species i, $R_i$is the net rate of production of species *i* by chemical reaction, S_i is the rate of creation by addition from the dispersed phase plus any user-defined sources, and $\vec{J_i}$is the diffusion flux of species *i*.

3.5. Combustion model

This model has been combined with species transports and the finite rate chemistry with the simplified reactions of the chemistry for simulating the general process of combustion in the diesel engines. This technique has been modeled on the basis of the solution of transport equations regarding the species mass fractions. Also, the rates of the reaction emerging as source terms in the equations of the species transport were assessed from the common expressions of the Arrhenius rate [24-26].

Arrhenius rate equation

$$\dot{R}_{i,r} = \Gamma(\ddot{\upsilon}_{i,r} - \acute{\upsilon}_{i,r})(K_{f,r} \prod_{j=1}^{N} [C_{j,r}]^{\acute{\eta}_{j,r}} - k_{b,r} \prod_{j=1}^{N} [C_{j,r}]^{\acute{\upsilon}_{j,r}}) \tag{4}$$

where Γ represent the net impact of 3rd bodies on the rate of the reaction. This term can be represented as:

$$\Gamma = \sum_j^N \gamma_{j,r} C_j \tag{5}$$

where $\gamma_{j,r}$ represents a 3rd body efficiency of *j*-th species in the *r*-th reaction, *r* is reaction, $\ddot{\upsilon}_{i,r}$ is stoichiometric coefficient for reactant *i* in reaction *r*, $\acute{\upsilon}_{i,r}$ is stoichiometric coefficient for product *i* in reaction *r*, $k_{b,r}$ is backward rate constant for reaction *r*, $\acute{\eta}_{j,r}$ is the rate exponent for reactant species *j* in reaction *r*, and *N* is number of chemical species in the system

$$k_{f,r} = A_r T^{\beta r} e^{-E_r/_{RT}} \tag{6}$$

where A_r represents a pre exponential factor (consistent units), E_r represents activation energy for the reaction (J/kg.mol), *R* represents a universal gas constant (J/kgmol-K), $k_{f,r}$ is forward rate constant for reaction *r*, and B_T is temperature exponent (dimensionless).

3.6. Air-fuel ratio and lambda value (λ)

The air-fuel ratio (AFR) is a major component that influences engine performance. The air-fuel ratio (AFR) is the ratio of the mass of air to the mass of fuel that the engine uses when it is running. The stoichiometric AFR is the minimal amount of air required for the complete combustion of fuel. Internal combustion engines do

not operate at optimum stoichiometric AFR, but rather at values near to it. As a result, we will have both an actual and ideal air-fuel AFR. The ratio between the actual air-fuel ratio (AFRactual) to the stoichiometric air-fuel ratio (AFRideal) is called lambda (λ).

$$\text{lambda}(\lambda) = \frac{(\text{Air/Fuel})\text{Actual}}{(\text{Air/Fuel})\text{stoichiometric}} \tag{7}$$

where λ = 1: stoichiometric, λ < 1: rich mixture-air deficiency, and λ > 1: lean mixture-excess air

$$\text{AFR (stoichiometric)} = \frac{ma}{mf} \tag{8}$$

where AFR stoichiometric is the air-fuel ratio, *ma* is the mass of air, and *mf* is the mass of fuel, and $\boldsymbol{\lambda}$ is lambda

A lean air-fuel blend has a high percentage of air and a small percentage of fuel. A slightly lean blend is good for reducing fuel usage and pollutants. Adding more air to the cylinder causes full combustion, which means that all the fuel is consumed. If the mixture is too lean, problems such as loss of power and even engine damage may develop. In contract, a rich air-fuel mixture has a high proportion of fuel and a low proportion of air. Excessively rich mixtures can lead to decreased engine output and incomplete combustion. This study focused on investigating mixing ratios, combustion characteristics, and pollution from diesel-syngas dual fuel under 1 lambda value.

3.7. Initial and boundary conditions

The initial pressure, and the temperature inside the engine cylinder during the intake stroke are 100,000 pa and 330°C, respectively. But, to save time, the simulation was performed during strokes of compression and combustion. The calculations start at 310º crank angle degrees prior to TDC for simulation and stop at 420º following TDC, which covers the compression stroke, combustion process, and fuel injection process. Also, the initial pressure, as well as the temperature within the engine cylinder, must be specified for providing initial conditions in terms of the governing equations to be solved. In addition, the temperature was 800 C at a crank angle of 340, while the initial pressure is 20000000 Pa. The time step utilized for each crank angle degree for the processes was 0.25, indicating that four-time steps are going to be required for calculating one crank angle degree. The reason for selecting the small-time steps was for avoiding the negative densities happening throughout the calculation [23].

3.8. Grid generation.

The mesh domain of combustion chamber was created by using a structured mesh that consists of hexahedral and tetrahedral mesh elements. The Grid independence examination for mesh was prepared for the Ricardo Hydra diesel engine model. The three-size different meshes had been created as described in Fig. 1 and Table 4. At an engine speed of 2000 rpm and the syngas substitution ratio with diesel of 30%, the simulation was done for each mesh to illustration independence. Figure 2 indicates the estimated cylinder pressure maximum inside the combustion chamber. The results were apparent that there is no marked difference between the three-size different meshes. Indeed, the refined mesh raises the CPU costs by three times and meanwhile has not been given beneficially for the simulation of the CFD.

Therefore, considering the computational time, case 2 has been selected as the most appropriate for the present research.

Table 4. Nodes and elements ratio utilized for GIT.

Cases	Elements	Nodes
Case 1	149203	139628
Case 2	323587	399886
Case 3	488431	509382

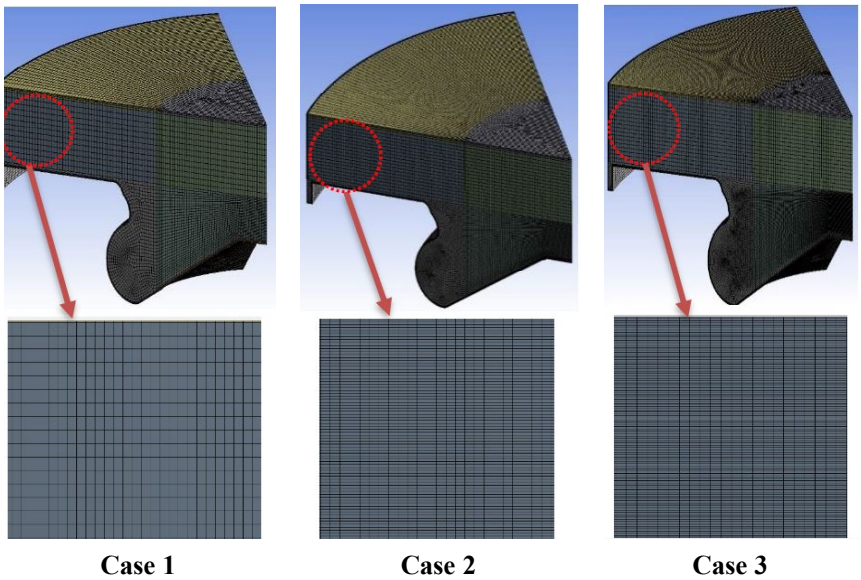

Fig. 1. The three-size different meshes.

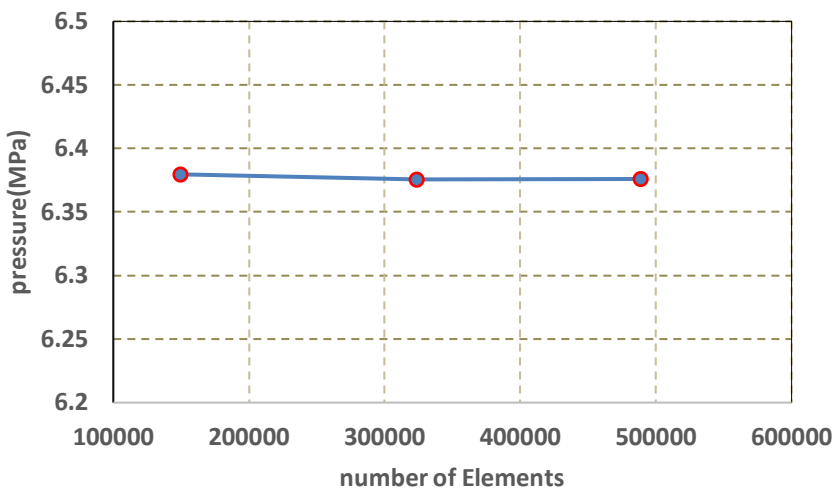

Fig. 2. Grid independence examination results.

4. Results

There are 5 addition ratios that are utilized for studying the impact of adding syngas on the combustion properties of diesel fuel. The impact of adding syngas on the combustion properties of the diesel engine and identify the maximum possible addition rate without occurring knocking or autoignition inside the engine have been evaluated by the use of ANSYS workbench 16.1. The simulation results on combustion characteristics of the mixture were analyzed as shown below.

4.1. Pressure

Figure 3 summarizes the relationship between the crank angle and pressure inside the engine cylinder under different addition ratios. Figure 4 summarizes the effects of altered mixtures of syngas fuel on peak in-cylinder pressure under different addition ratios. The data in Figs. 3 and 4 show an improvement in the peak pressure with syngas in addition to diesel fuel. Moreover, the values of maximum pressure are enhanced from 3649131Pa (360 degree) at diesel mode to 5219543pa (372 degree), 6241979pa (373 degree), 6375614 pa (373.4 degree) , and 6459573 pa (373.5 degree) under dual fuel mode with addition ratios of (20%, 30%,40%, and 50%) respectively. In addition, the maximum possible addition rate without occurring knocking or autoignition inside the engine is 50%. The syngas consists of 50% hydrogen and 50% CO. Hydrogen is a light gas and has a faster ignition and higher flame speed. Therefore, an increase of hydrogen fraction in the blend of fuel (diesel -syngas) leads to an increase in-cylinder pressure and temperature due to the high content of specific energy and considerably faster flame. By contrast, the peak in-cylinder pressure decreased as the diesel fuel fraction increased due to the low flammability of the diesel fuel.

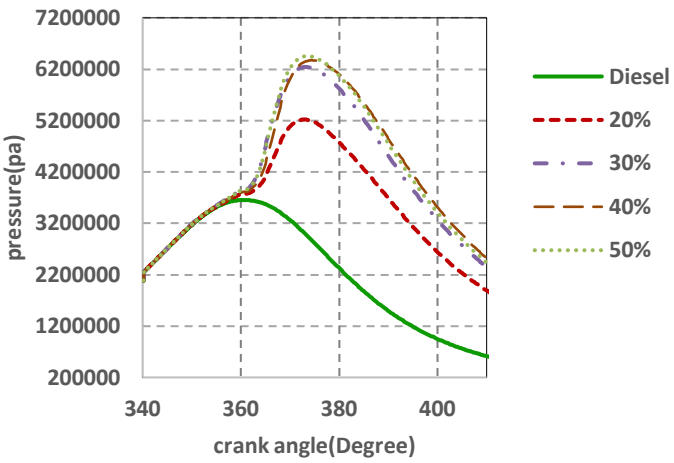

Fig. 3. In-cylinder pressure curves under different addition ratios.

Figure 5 displays the pressure contours of altered mixtures under different addition ratios and lambda value is 1. Figure 5 also illustrates that the pressures inside the engine increased with the increasing the replacement ratio of syngas with diesel and it reached its maximum rate in the Diesel-syngas dual mode under replacement ratio is 50%.

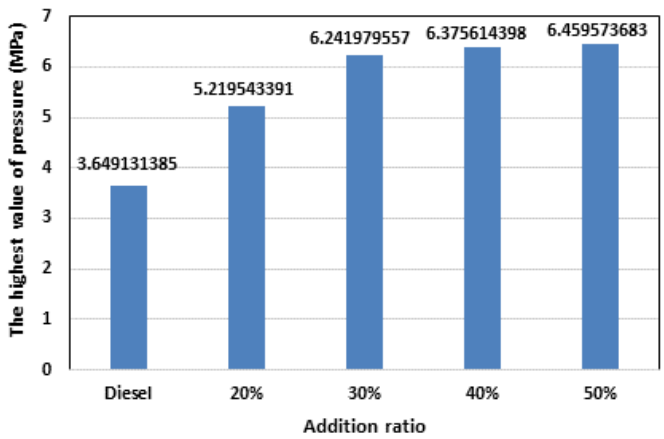

Fig. 4. Maximum value of pressure inside the engine at different addition ratios and 1 lambda value.

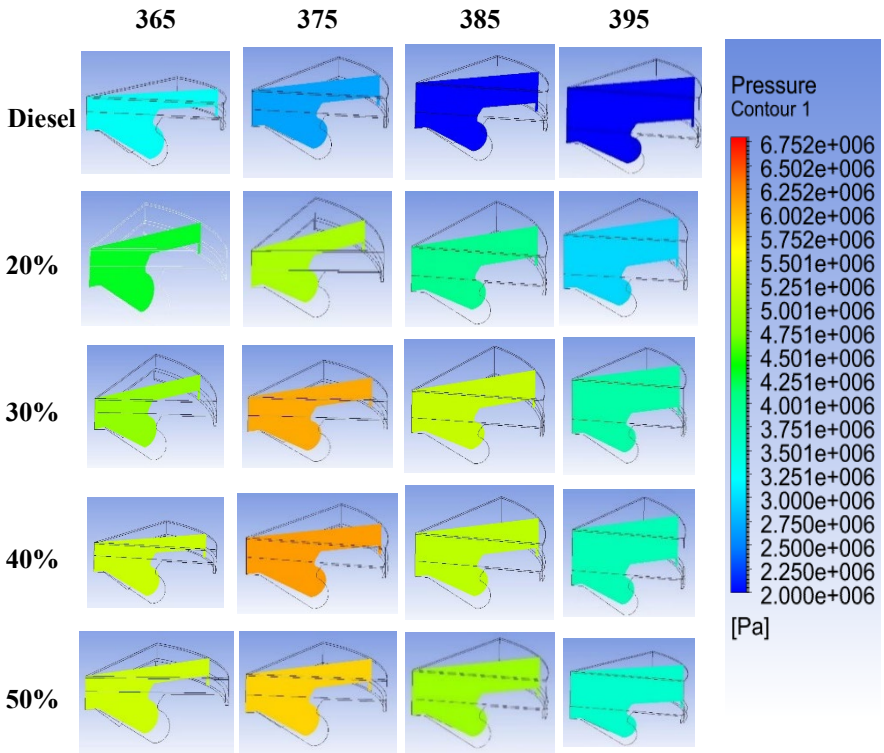

Fig. 5. Average pressure development under different addition ratios.

4.2. Temperature

Figure 6 summarizes the relationship between the crank angle and temperature inside the engine cylinder under different addition ratios. Figure 7 summarizes the effects of altered mixtures of syngas fuel on peak in-cylinder temperature under different addition ratios. As explained in Figs. 6 and 7, the in-cylinder temperature

increases with increase of addition ratios. Moreover, the values of the maximum temperature inside the cylinder are improved from 913K at diesel mode to 1950K, 2424K, 2626K, and 2755K under dual fuel mode with addition ratios of (20%, 30%,40%, and 50%) respectively. In addition, the maximum possible addition rate without occurring knocking or autoignition inside the engine is 50%. Because the syngas consists of 50% hydrogen and 50% CO. The hydrogen has a fast-burning level, which in turn, leads to the high combustion temperature for the mixture. On the other hand, the peak in-cylinder temperature at diesel fuel mode decreased because of the low flammability of diesel combustion.

Figure 8 displays the temperature contours of altered mixtures under an engine speed of 2,000 rpm and lambda value of 1. Figure 8 also reveals that the combustion temperature and its formation area improved with the addition of syngas to diesel fuel.

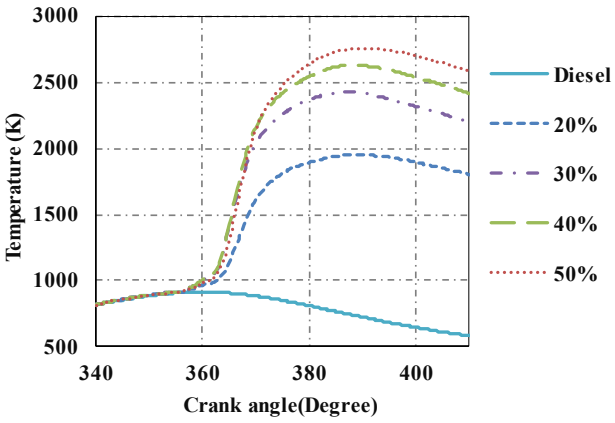

Fig. 6. In-cylinder temperature curves under different addition ratios.

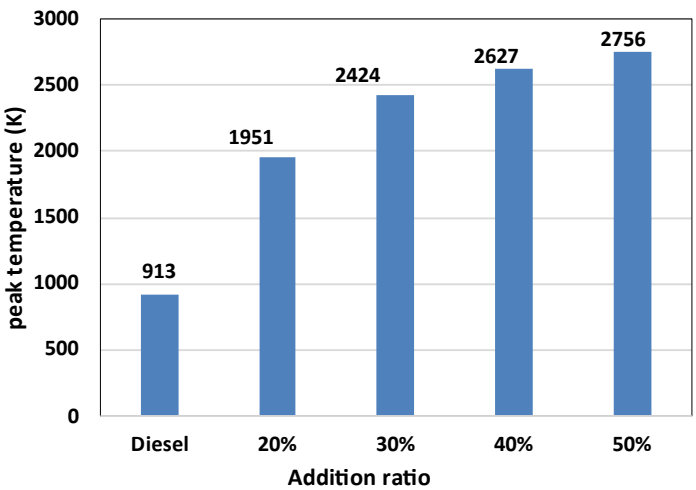

Fig. 7. Maximum value of temperature inside the engine at different addition ratios and 1 lambda value.

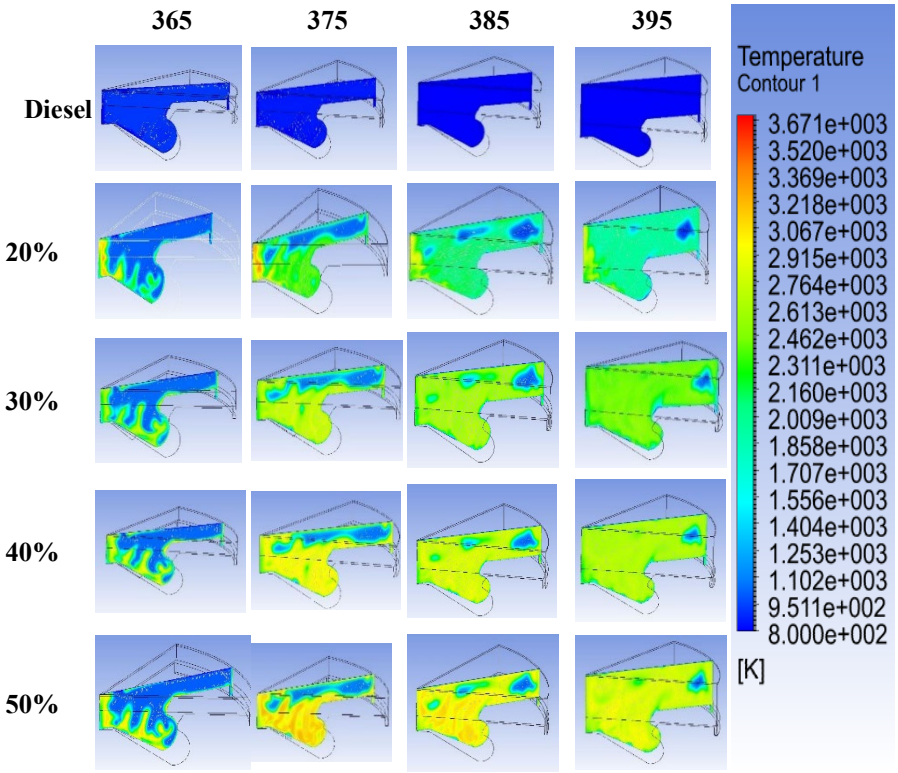

Fig. 8. The development of the average temperature under different addition ratios.

4.3. Carbon monoxide emission (CO)

Figure 9 summarizes the relationship between the crank angle and CO development inside the engine cylinder under different addition ratios. Figure 10 summarizes the effects of altered mixtures of syngas fuel on high values of CO emissions inside the engine cylinder.

As seen in Figs. 9 and 10, when the substitution ratio of syngas to diesel rises, the CO concentration in the fuel-air blend increases rapidly inside the engine, thereby raising the peak co pollution. This is due to the fact that the syngas consists of 50% hydrogen and 50% CO. Therefore, increasing the syngas addition to diesel -syngas dual-fuel engine increases the syngas fraction in the mixture in turn raising the CO emission.

Figure 11 shows the formation regions of CO under different addition ratios for syngas with diesel at 2000 rpm and 1 lambda value. As depicted in Fig. 11, increasing diesel fraction has eliminated the formation of CO. This is due to the fact that the ratios of CO emissions of diesel engines are so small that can be ignored [19, 23]. Moreover, the syngas consists of 50% hydrogen and 50% CO. Therefore, increasing the addition ratios under dual-fuel engine increases the syngas fraction in the mixture in turn raising the co emission.

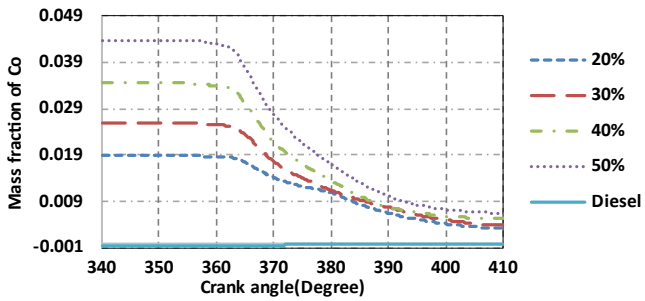

Fig. 9. Curves of in-cylinder CO under different addition ratios.

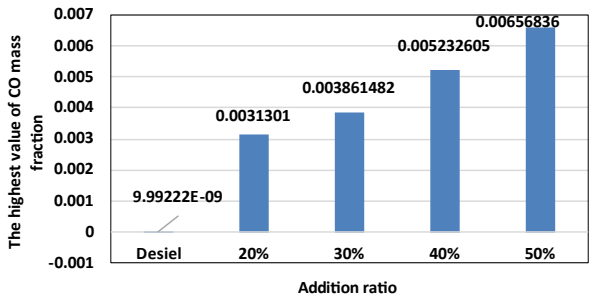

Fig. 10. Maximum value of CO emission inside the engine at different addition ratios and 1 lambda value.

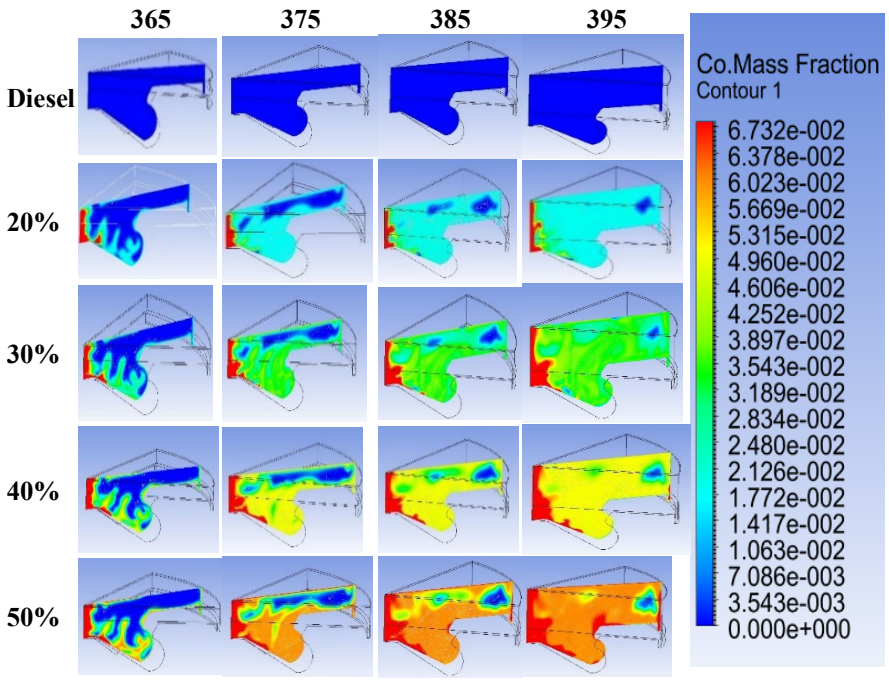

Fig. 11. The development of CO mass fraction of pollutant under different addition ratios.

4.4. Carbon dioxide emission (CO_2)

Figure 12 summarizes the relationship between the crank angle and CO_2 development inside the engine cylinder under different addition ratios. Figure 13 summarizes the effects of altered mixtures of syngas fuel on high values of CO_2 emissions inside the engine cylinder under different addition ratios. As seen in Figs. 12 and 13, when the addition ratios rise, the in-cylinder CO_2 emissions concentration increases rapidly inside the engine. Figure 14 shows the formation regions of CO_2 under different addition ratios. As depicted in Fig. 14, increasing the diesel fraction has eliminated the formation of CO_2.

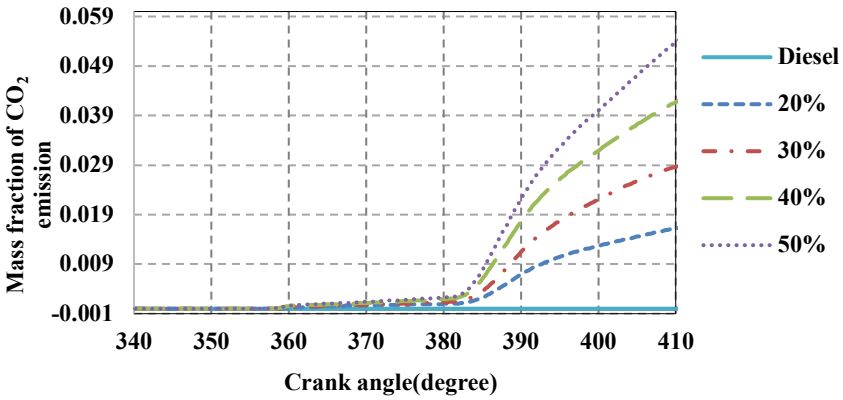

Fig. 12. In-cylinder CO_2 emission curves under different addition ratios.

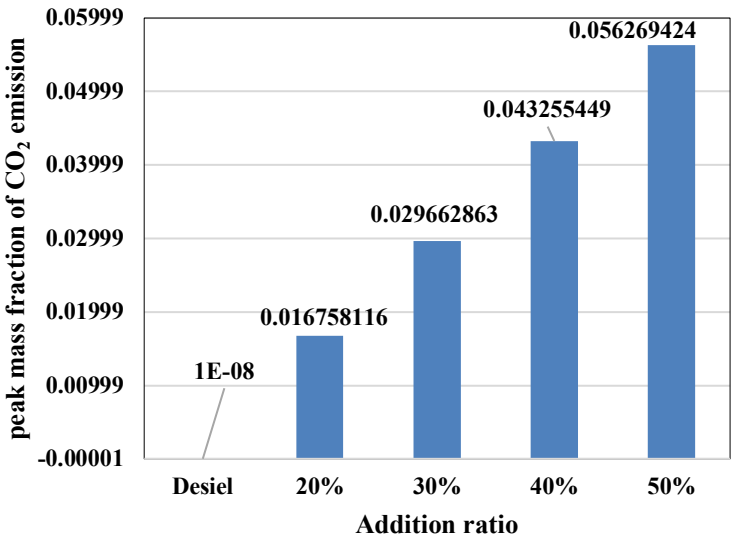

Fig. 13. The maximum value of CO_2 emission inside the engine at different addition ratios and 1 lambda value.

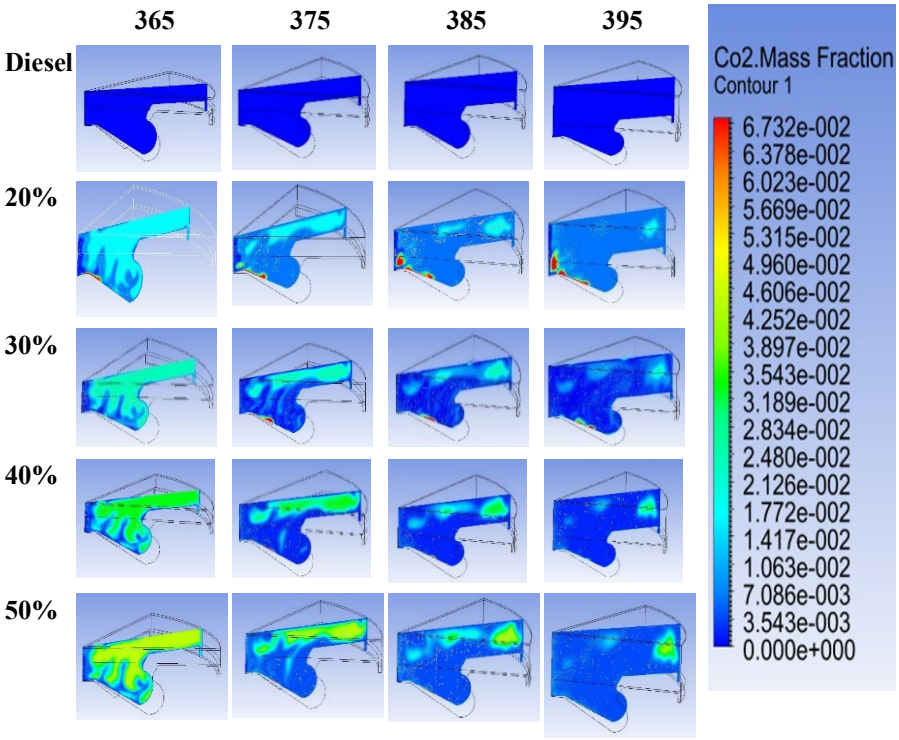

Fig. 14. The development of carbon dioxide mass fraction under different addition ratios.

4.5. Nitric oxide emission (NO)

Figure 15 summarizes the relationship between the crank angle and NO development inside the engine cylinder under different addition ratios. Figure 16 summarizes the effects of altered mixtures of syngas fuel on high values of nitric oxides emissions inside the engine cylinder under different addition ratios, 2000 rpm engine speed, and 1 lambda value. As seen in Figs. 15 and 16, when the substitution ratio of syngas to diesel rises, the hydrogen concentration in the fuel-air blend increases rapidly inside the engine, thereby raising the peak NO pollution. Figure 17 shows the formation regions of NO under different addition ratios. As depicted in Fig. 17, increasing diesel fraction has eliminated the formation of NO due to low temperature of diesel combustion.

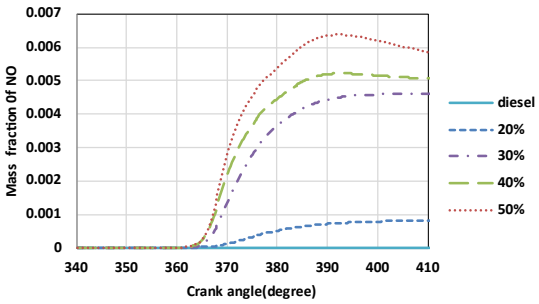

Fig. 15. Curves of in-cylinder NO under different addition ratios.

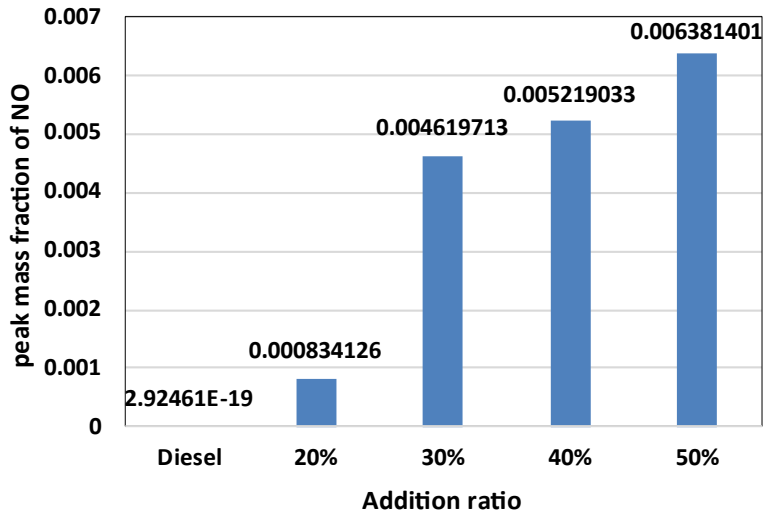

Fig. 16. Maximum value of NO emission inside the engine at different addition ratios and 1 lambda value.

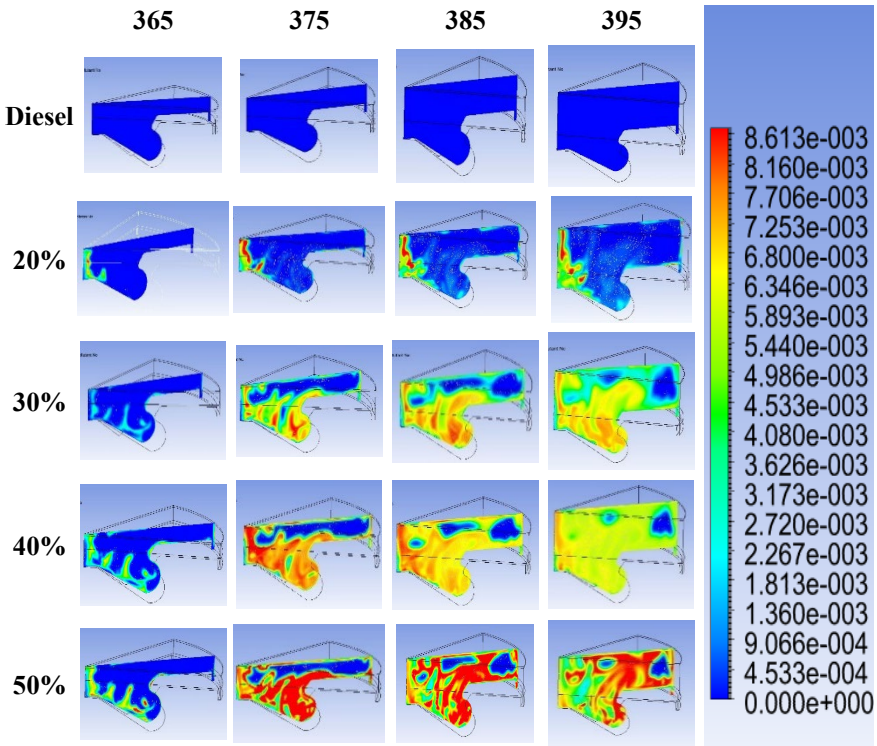

Fig. 17. The development of NO mass fraction under different addition ratios.

5. Conclusions

The current study contributed to the knowledge of the combustion and emission characteristics for the syngas-Diesel dual-fuel engine under different addition ratios (20%,30%,40%, and 50%) and lambda value of 1. The current study utilized a single-cylinder direct injection method to investigate the influence of employing diesel with syngas using Computational Fluid Dynamics at different addition ratios within a diesel engine at engine speed 2000 rpm and 1 lambda value. From the simulation outcomes, the following conclusions are obtained.

- In comparison to a dual-fuel engine (syngas-diesel), the emission rates of NO, CO_2, and CO from a diesel engine are relatively low. Besides, referring to numerical results, the emissions of NO, CO_2, and CO within the engine raised when the addition ratios in the dual-fuel mode raised compared to diesel engine emissions.
- Based on simulation findings, the values of NO mass fraction are rised from 2.45904E-24 at diesel mode to 3.21152E-18 (20%), 4.05245E-18 (30%), 4.90555E-18 (40%) and 5.63127E-18 (50%). Furthermore, ratios of the CO_2 mass fraction are raised from 1E-08 at diesel mode to 0.016758116, 0.029662863, 0.043255449and 0.056269424 under a syngas-diesel dual fuel mode with addition ratios of 20%, 30%, 40%, and 50%, respectively. Moreover, the ratios of CO mass fraction are increased from 9.99222E-09 at diesel mode to 0.0031301, 0.003861482, 0.005232605and 0.00656836 under a syngas-diesel dual fuel mode with addition ratios of (0%, 20%, 30% ,40% and 50%) respectively.
- With the increment of the syngas ratio, the combustion performance of the diesel engine was enhanced. In comparison with the five instances of addition ratios, the diesel engine generates the minimum temperature and pressure in-cylinder under a diesel-syngas dual engine. Besides, pressure and temperature in the engine enhanced as the addition ratios of syngas with diesel raised. In addition, the maximum possible addition rate without occurring knocking or autoignition inside the engine is 50%.
- Based on numerical outcomes, the values of the maximum temperature inside the cylinder are improved from 913K at diesel mode to 1950K, 2424K, 2626K, and 2755K under dual fuel mode with addition ratios of (20%, 30%,40%, and 50%) respectively. Moreover, the values of maximum pressure are enhanced from 3649131Pa at diesel mode to 5219543pa, 6241979pa, 6375614 pa and 6459573pa under dual fuel mode with addition ratios of (20%, 30%,40%, and 50%) respectively. In addition, the maximum possible addition rate without occurring knocking or autoignition inside the engine is 50%.

Nomenclatures

A_r	A pre exponential factor, consistent units
B_T	Temperature exponent, dimensionless
Er	Activation energy for the reaction, J/kg.mol
$\vec{J}_i$	The diffusion flux of species i
$k_{b,r}$	Backward rate constant for reaction r
$k_{f,r}$	Forward rate constant for reaction r
$\acute{m}_D$	The mass flow rate for diesel, kg/s
$\acute{m}_s$	The mass flow rate for the syngas, kg/s

N	Number of chemical species in the system
R	A universal gas constant, J/kgmol-K
R_i	The net rate of production of species i by chemical reaction
Sct	Turbulent Schmidt number
S_i	The rate of creation by addition from the dispersed phase plus Any user-defined sources.
S_{ig}	Source term for the ignition species
Yi	Mass fraction of a chemical species I, dimensionless
Yig	Mass fraction of a radical species, dimensionless
Greek Symbols	
$\gamma j,r$	A 3rd body efficiency of j-th species in the r-th reaction.
Γ	The net impact of 3rd bodies on the rate of the reaction
ρ	The flow density, kg/m^3
λ	Lambda
v	The Absolute velocity vector, m/s
$\acute{\upsilon}_{i,r}$	Stoichiometric coefficient for product i in reaction r
$\ddot{\upsilon}_{i,r}$	Stoichiometric coefficient for reactant i in reaction r
μt	Viscosity, Pa.s
Γ	Temperature exponent, dimensionless
$\acute{\eta}_{j,r}$	Rate exponent for reactant species j in reaction r
Abbreviations	
AFR	Air-fuel ratio
AFRactual	The actual air-fuel ratio
AFRideal	The stoichiometric air-fuel ratio
CFD	Computational fluid dynamics
CH_4	Methane
CI	Compression ignition
CNG	Compressed natural gas
CO	Carbon monoxide
CO_2	Carbon dioxide
CR	Compression ratio
DDF	Diesel dual fuel
DF	Dual-fuel
GIT	Grid independent test
H_2	Hydrogen
H_2O.	Water
HC	Hydrocarbon
HCNG	Blend of hydrogen and Compressed natural gas
ICE	Internal combustion engine
kε	k-epsilon
LHVD	The lower heating values of diesel (MJ/kg)
LHVs	The lower heating values of syngas (MJ/kg)
LNG	Liquefied natural gas
LPG	Liquefied petroleum gas
r	Reaction
RNG	Re-Normalisation Group
UD	Upwind differencing

References

1. Çeper, B.A. (2012). *Use of hydrogen-methane blends in internal combustion engines*. InTech: London, UK.
2. Dhole, A.E.; Yarasu, R.B.; Lata, D.B.; and Priyam, A. (2014). Effect on performance and emissions of a dual fuel diesel engine using hydrogen and producer gas as secondary fuels. *International Journal of Hydrogen Energy*, 39(15), 8087-8097.
3. Minic, D. (2012). *Hydrogen energy - Challenges and perspectives*. InTech: London, UK
4. Karagöz, Y.; Güler, İ.; Sandalcı, T.; Yüksek, L.; Dalkılıç, A.S.; and Wongwises, S. (2016). Effects of hydrogen and methane addition on combustion characteristics, emissions, and performance of a CI engine. *International Journal of Hydrogen Energy*, 41(2), 1313-1325.
5. Dzombo, D.M.; Kiplimo, R.; and Kiplagat, J.K. (2013). Use of biomass gas in running internal combustion engine to generate electricity - A review. *Proceedings of Sustainable Research and Innovation Conference*, 89-95.
6. Alhamdany, A.A.; Hameed, A.Q.; and Salman, Q.M. (2018). Experimental investigation for the removal of toxic gases from vehicle exhaust using non-thermal plasma. *Journal of Engineering*, 24(8),55-70.
7. Pichayapat, K.; Sukchai, S.; Thongsan, S.; and Pongtornkulpanich, A. (2014). Emission characteristics of using HCNG in the internal combustion engine with minimum pilot diesel injection for greater fuel economy. *International Journal of Hydrogen Energy*, 39(23), 12182-12186.
8. Danardono, D.; Kim, K.S.; Lee, S.Y.; and Lee, J.H. (2011). Optimization the design of venturi gas mixer for syngas engine using three-dimensional CFD modeling. *Journal of Mechanical Science and Technology*, 25(9), 2285-2296.
9. Hagos, F.Y.; Aziz, A.R.A.; and Sulaiman, S.A. (2013). Study of syngas combustion parameters effect on internal combustion engine. *Asian Journal of Scientific Research*, 6(2), 187-196.
10. Mahgoub, B.K.M.; Hassan, S.; and Sulaiman, S.A. (2015). Effect of varying engine parameters and syngas composition on the combustion characteristics, performance and emission of syngas-diesel dual fuel engine - A review. *ARPN Journal of Engineering and Applied Sciences*, 10(17), 7712-7718.
11. Ali, A.A.M.M.; Ali, K.; Kim, C.; Lee, Y.; Oh, S.; and Kim, K. (2019). Numerical study of the combustion characteristics in a syngas-diesel dual-fuel engine under lean condition. *International Journal of Automotive Technology*, 20(5), 933-942.
12. Piazzullo, D.; Costa, M.; Petranovic, Z.; Vujanovic, M.; La Villetta, M.; Caputo, C.; and Cirillo, D. (2018). CFD modelling of a spark ignition internal combustion engine fuelled with syngas for a mCHP system. *Chemical Engineering Transactions*, 65,13-18.
13. Feng, S. (2017). Numerical study of the performance and emission of a diesel-syngas dual fuel engine. *Mathematical Problems in Engineering*, Volume 2017 |Article ID 6825079, 1-12.
14. Azimov, U.; Okuno, M.; Tsuboi, K.; Kawahara, N.; and Tomita, E. (2011). Multidimensional CFD simulation of syngas combustion in a micro-pilot-

ignited dual-fuel engine using a constructed chemical kinetics mechanism. *International Journal of Hydrogen Energy*, 36(21),13793-13807.

15. Stylianidis, N.; Azimov, U.; Maheri, A.; Tomita, E.; and Kawahara, N. (2017). Chemical kinetics and CFD analysis of supercharged micro-pilot ignited dual-fuel engine combustion of syngas. *Fuel*, 203, 591-606.
16. Mahmood, H.A.; Adam, N.M.; Sahari, B.B.; and Masuri, S.U. (2017). New design of a CNG-H_2-air mixer for internal combustion engines: An experimental and numerical study. *Energies*, 10(9), 1-27.
17. Mahmood, H.A.; Adam, N.M.; Sahari, B.B.; and Masuri, S.U. (2018). Development of a particle swarm optimisation model for estimating the homogeneity of a mixture inside a newly designed CNG-H_2-AIR mixer for a dual fuel engine: An experimental and theoretic study. *Fuel*, 217, 131-150.
18. Mahmood, H.A.; Adam, N.M.; Sahari, B.B.; and Masuri, S.U. (2017). Design of compressed natural gas-air mixer for dual fuel engine using three-dimensional computational fluid dynamics modeling. *Journal of Computational and Theoretical Nanoscience*, 14(7),3125-3142
19. Alrazen, H.A.; Talib, A.A.; and Ahmad, K.A. (2016). A two-component CFD studies of the effects of H_2, CNG, and diesel blend on combustion characteristics and emissions of a diesel engine. *International Journal of Hydrogen Energy*, 41(24), 10483-10495.
20. Wannatong, K.; Akarapanyavit, N.; Siengsanorh, S.; and Chanchaona, S. (2007). Combustion and knock characteristics of natural gas diesel dual fuel engine. *SAE Technical Paper*, 1(2047),1-6.
21. Hagos, F.Y.; Aziz, A.R.A.; and Sulaiman, S.A. (2014). Trends of syngas as a fuel in internal combustion engines. *Advances in Mechanical Engineering*, 6, 1-10.
22. Köse, H.; and Ciniviz, M. (2013). An experimental investigation of effect on diesel engine performance and exhaust emissions of addition at dual fuel mode of hydrogen. *Fuel Processing Technology*, 114, 26-34.
23. Ali, R. ; Raheemah, S.H. ; and Al-Mayyahi, N.N. (2020). Numerical analysis of combustion characteristics and emission of dual and tri-fuel diesel engine under two engine speeds. *Jordan Journal of Mechanical and Industrial Engineering*, 14(2), 205-213.
24. Fluent, A. (2012). 14.5 *User Guide*. Canonsburg, Pennsylvania, USA.
25. Fluent, F. (2006). 6.3 *user's guide*. Fluent Inc.
26. Manual, U. (2009). *ANSYS FLUENT* 12.0. Theory Guide.
27. Belal, T.M.; Marzouk, E.M.; and Osman, M.M. (2013). Investigating diesel engine performance and emissions using CFD. *Energy and Power Engineering*, 5(2), 171-180.
28. Hardenberg, H.O.; and Hase, F.E. (1979). An empirical formula for computing the pressure rise delay of a fuel from its cetane number and from the relevant parameters of direct-injection diesel engines. *SAE Transactions*, 88(2), 1823-1834.